Micro-scale Interactions between Chemotactic Bacteria and Algae

by

Nisha Vahora

B.S. Environmental Engineering
Massachusetts Institute of Technology, 2008

Submitted to the Department of Civil and Environmental Engineering in Partial Fulfillment of the Requirements for the Degree of

Master of Engineering in Civil and Environmental Engineering
at the
Massachusetts Institute of Technology

June 2010

Signature of Author: _____

Department of Civil and Environmental Engineering
May 20, 2010

Certified by: _____

Martin F. Polz
Professor of Civil and Environmental Engineering
Thesis Supervisor

Certified by: _____

Roman Stocker
Associate Professor of Civil and Environmental Engineering

Accepted by: _____

Daniele Veneziano
Chairman, Departmental Committee for Graduate Students

Micro-scale Interactions between Chemotactic Bacteria and Algae

by

Nisha Vahora

Submitted to the Department of Civil and Environmental Engineering on May 20, 2009 in partial fulfillment of the requirements for the Degree of Master of Engineering in Civil and Environmental Engineering

Abstract

Traditional views of marine environments describe the ocean pelagic zone as a homogeneous nutrient-poor environment. Heterotrophic marine bacteria that have evolved high-energy mechanisms for swimming abilities and sensing nutrient gradients would gain no survival advantage under this model. Recent identification of microscale (<1cm) nutrient patches, such as those produced by algal exudates, explain a potential for these evolved functions. With this new model for the pelagic zone, bacteria, through chemotaxis and motility, can sense and respond to microscale carbon patches exuded from growing algae. This study examines possible conditions necessary under which it is advantageous to swim. As an initial step to test this hypothesis, we developed a system to investigate bacterial chemotaxis to algal exudates. Two algae from the genus, *Thalassiosira*, which differed in size, were grown in artificial seawater and filtered, with the use of a novel instrument, to generate nutrient heterogeneity at the microscale. *Pseudoalteromonas haloplanktis* was added to algal cultures with varying algae:bacteria ratios of 1:250 to 1:50,000 and bacterial chemotaxis was observed by localization around individual algae. *P. haloplanktis* exhibited chemotaxis towards the larger algae *Thalassiosira rotula* within seconds but not *Thalassiosira weissflogii* suggesting larger algae elicit a chemotactic response. Results provide evidence of real time clustering in response to the presence of live algae and suggest a mechanism that provides a fitness advantage over non-motile bacteria.

Thesis Supervisor: Martin F. Polz
Titles: Professor of Civil and Environmental Engineering

Thesis Supervisor: Roman Stocker
Titles: Associate Professor of Civil and Environmental Engineering

Acknowledgements

I would first like to thank my advisors Martin Polz and Roman Stocker, for their continual support. Their thoughtful guidance was an invaluable resource that aided me along the ever evolving path of my research. Their continuous excitement and dedication has inspired me to continue similar research and will no doubt propel my career for years to come. I would also like to thank my lab mates over the past year. Their companionship at the lab bench helped me get through the long nights and road blocks along the way. Special thanks to Hans Wildschutte for his help steering my experiments down the right path and Marcos and Tanvir Ahmed for their help in becoming a skilled user of the Stocker Lab microscope. Further thanks to my friends and family who have put up with my scientific pursuits over the past year. I will continue to rely on their support in the years to come.

Contents

List of Figures

List of Tables

1 Introduction

In the ocean, carbon is fixed through photosynthesis into organic matter that serves as nutrient fuel for the marine food web. Half of the fixed carbon is directed via marine bacteria into the microbial loop (Pomeroy et al., 2007), a major pathway for organic matter flux (Azam et al., 1983; Cole et al., 1988; Fuhrman and Azam, 1982). Past research has defined the pelagic zone in the ocean to be nutrient poor, where fixed carbon released by algae (through algal exudates) contribute to the homogenous low bulk nutrient concentrations and is remineralized by bacteria. But, recent studies suggest higher nutrient concentrations are present at the microscale at any point in time. Over time, the spatial nutrient profile changes due to creation and utilization of nutrient sources. Algal exudates are present in small but abundant patches that can be quickly dissipated due to diffusion and turbulence in the ocean. This suggests the relationship between bacteria and algae to be more complex than the classical view.

The patchy environment of the ocean poses a different survival challenge for marine bacteria as compared to the well-studied strain *Escherichi coli*, the primary lab model used to define many microbial processes. These enteric bacteria reside in a nutrient-replete environment where exposure to nutrients is not limited. In the pelagic zone, bacteria either need to survive on low but steady nutrient concentrations in the water, or need to exploit nutrient patches, which are ephemeral and thus require the ability to survive a highly variable environment (Polz et al., 2006). How does the efficiency of bacterial utilization of these nutrient patches influence the biogeochemical transformation rates in the ocean? Bacteria may gain a growth advantage through the ability to exploit these nutrient patches before they dissipate through motility and chemotaxis (Blackburn et al., 1998). On the other hand, swimming incurs a cost that offsets this advantage, and this cost is particularly large at small scales, where swimming efficiency is on the order of 1% (Mitchell, 1991).

This thesis investigates the micro-scale interactions between phytoplankton and chemotactic bacteria that occur on the scale of a nutrient patch. This environment enriched with media surrounding an algal cell is termed phycosphere and is an example of an aquatic microenvironments, defined as having local resource inhomogeneities on scales within the dispersal range of individuals.

1.1 Micro-scale Heterogeneity in the Ocean

Historically, large spatial-scale studies have been conducted to characterize nutrient profiles (both lateral and vertical) in the ocean. Although traditional methods (e.g. Niskin bottles) of collecting seawater samples have aided in the confirmation of an oligotrophic pelagic environment, the environment at the micro-scale is significantly different. These microenvironments (scale of 1cm or less) are defined by patches or microaggregates of high levels of nutrients and biomass (Figure 1.1). Examples of these nutrients include phytoplankton photosynthetic products such as algal exudates (Bowen et al., 1993; Mitchell et al., 1985), zooplankton excretion (Lehman and Scavia, 1982), cell lysate (Blackburn et al., 1998), and organic mater leaking from particles (Kiorboe and Jackson, 2001). Studies have estimated these patches contain nutrients two to three orders of magnitude above that of the surrounding seawater (Blackburn et al., 1997; Blackburn et al., 1998; Kiorboe and Jackson, 2001).

Goldman explains that although total volume of these microaggregates would be small in comparison with the total volume of the water column, the nutrient concentrations and active biomass in the microaggregates would be significantly higher (Goldman, 1984). Existence of these microaggregates is further supported by observations of bacterial clustering around single marine alga cells (Blackburn et al., 1998) and increased bacterial abundance in natural sweater samples at the mm scale (Seymour et al., 2000; Seymour et al., 2004) .

Microorganisms that are able to associate with these aquatic microenvironments may have a significant growth advantage and survival capacity in an overall oligotrophic open-ocean.

1.2 Living in Aquatic Microenvironments

In these aquatic microenvironments, fluid dynamics influence the condition microbes live in and potential interaction with nutrient sources. The Reynolds Number, a dimensionless number that is the ratio of inertial forces to viscous forces, describes the relative importance of inertial and viscous forces. At the micro-scale, Reynolds Number is approximately between $10^{-5} - 10^{-4}$. Because the Reynolds Number is low for heterotrophic bacteria, the local aqueous environment around the cell is carried along as the cell swims with viscous forces dominating. The Peclet number, Pe, describes the ability of the microorganism to shake off the water that immediately surrounds it (Tennekes and Lumley, 1972):

$$Pe = \frac{\ell v}{D}$$

ℓ, length of interest
v,swimming speed
D, diffusion coefficient

In water, at the microscale, typical values are =10 μm, =20 - 30 μm/s, and . With these values, Pe will be less than 1 and transport of nutrients occur primarily by diffusion, which also dominates cell movement.

Bacterial chemotaxis may be adaptive if it affords the ability to take advantage of nutrient rich sources within aquatic microenvironments (Purcell, 1977). Due to the low Peclet number, a cell lacks the ability to exit its microscale environments. Within a microenvironment, a motile cell could take advantage of a diffusion-dominant state. To reach a nutrient-enriched point, marine bacteria would need to swim faster than it takes for the

nutrient point source to be affected completely by diffusion (Figure 1.2). (Jackson, 1989b). Mathematically, this is expressed as

$$\frac{D_N}{v} < \ell$$

D_N, diffusion constant of nutrient

With the ability to be motile, a cell has the capability to move to a nutrient-enriched zone within a microenvironment. If the cell could also direct its movement along a gradient, through a mechanism called chemotaxis, it has the potential to gain a growth advantage in a patchy environment.

1.3 Chemotaxis

The basic knowledge of bacterial motility is derived from the study of enteric bacteria. With the invention of the automatic tracking microscope in the 1970s, scientists were able to observe and study the rapid movement of motile bacteria (Berg, 1971). It was found that in an isotropic environment, a bacterium will swim in a straight line, called a run, then will either gradually or abruptly change its direction through tumbling, where a bacterium will flail around, or twiddle, where the bacterium will abruptly change its direction. It will then swim in a straight line, but in a semi-random new direction (Berg and Brown, 1972). In an anisotropic environment, where a chemoattractant is present, a bacterium will increase the length of a run, where they encounter and recognize an ascending gradient, or increase the number of tumbles, where they recognize a descending gradient (Berg and Brown, 1972; Macnab and Koshland, 1972). If a toxin or repellant is present, the bacterium will increase the number of tumbles, where there is an ascending gradient, or increase the length of a run, where there is a descending gradient (Tsang et al., 1973). The bacterium relies on

moving up and down gradients to recognize an ascending and descending trend because the cell is too small to sense a gradient across its own body length.

Cells have sensory devices called receptors that detect changes in chemical concentrations and signal the change to the flagella (Adler, 1969). It was hypothesized and later confirmed that flagella produce bacterial motion by rotating as rigid or semi-rigid helices (Berg and Anderson, 1973; Silverman and Simon, 1974). Runs are caused by counter-clockwise rotation of flagella and tumbling is caused from clockwise rotation (Larsen et al., 1974). Storage of information received by receptors results in a pseudo-memory that shapes their Biased Random Walk, ultimately moving in a desired direction, in contrast to the random movement observed in a homogeneous environment (Koshland, 1974).What substances in the environment posess chemotaxis-inducing effect to bring bacteria into a nutritious or less harmful environment (Adler, 1975)? There is not sufficient data to determine what exactly induces flagellar movement: whether it be a single or combination of chemical signal(s), potential energy from attractant, or something still to be discovered. (Chet and Mitchell, 1976). Energy costs are also very high, coming from the need to overcome fluid mechanical drag. This poses a cost-benefit situation to each cell where it needs to evaluate the cost of moving and the potential beneficial outcome.

1.3.1 Marine Chemotaxis

Results obtained by studying enteric bacterial swimming speeds and mechanisms are not accurately transferable to marine bacteria. Adler observed chemotactic enteric bacteria moving a few centimeters on a timescale of hours (Adler, 1975). In this case, $\frac{D_N}{v} > \ell$, and marine bacteria would not be able to take advantage of the nutrient patches through the use of an equivalent chemotaxis strategy. Due to the slow swimming speeds of enterics, the nutrient patch would dissipate before the cell could reach the nutrient-rich patch.

To exploit such nutrient patches, marine bacteria have a swimming behavior adapted to a changing environment and higher swimming speeds. Johansen et al. observed a modified swimming behavior from the run-and-tumble biased random walk (Johansen et al., 2002). It was reported that up to 70% of marine bacterial isolates observed demonstrated a run and reverse strategy. Instead of tumbling, marine bacteria would reverse their direction after each stop. This back and forth motion gave them the ability to form tight bands around chemoattractants. Compared to speeds up to 40 μm/s observed for enteric bacteria (Berg and Brown, 1972), swimming speeds up to and greater than 300 μm/s have been observed for marine bacteria (Barbara and Mitchell, 1996).

With the ability to swim and respond to ephemeral gradients faster, bacteria increase their ability to uptake nutrients. Blackburn et al. confirmed the hypothesis that marine bacteria could increase their nutrient uptake by taking advantage of algal nutrient releases. Bacteria were able to cluster around point sources and disperse once the source was fully utilized. The ability to steadily maintain a close but unattached association with a nutrient patch enables marine bacteria to move on once the nutrient source is depleted (Blackburn et al., 1998).

1.4 Microscale Interactions between Chemotactic Bacteria and Phytoplankton

In addition to observations and simulations of marine bacterial chemotaxis (Bell and Mitchell, 1972; Bowen et al., 1993; Jackson, 1987; Jackson, 1989a; Kiorboe and Jackson, 2001; Luchsinger et al., 1999), there are also new initiatives that have shown bacterial clustering around algal cells (Barbara and Mitchell, 2003a; Barbara and Mitchell, 2003b; Seymour et al., 2009). These cells serve as a nutrient point source due the phycosphere, the zone surrounding the cell that is enriched with the organic carbon the algae are producing

through photosynthesis and exuding (Bell and Mitchell, 1972). This zone serves as a nutrient rich source in aquatic microenvironments. It is important to note that other types of interactions between bacteria and algae can occur, in addition to the organic carbon coupling, as these could affect observations of their interaction. For example, bacteria can be competitors of algae for macronutrients such as phosphorus and nitrogen in a nutrient limited environment (Guerrini et al., 1998; Rhee, 1972) or symbionts of algae for example providing vitamin B12 to algal cells (Croft et al., 2005).

Barbara and Mitchell (2003) took an additional step and identified the spatial distribution of chemotactic marine bacteria in response to a nutrient point-source. By ionically bonding individual amino acids to ion exchange beads, the study compared the behavioral response of marine bacteria and enteric bacteria to nutrient point sources (Barbara and Mitchell, 2003b). Marine bacteria formed a discrete band (in tens of seconds) of cells at a fixed distance from the bead. This fixed distance is correlated to a preferred concentration gradient. Enteric bacteria did not duplicate this response.

Barbara and Mitchell, soon after the confirmation of bacterial clustering, observed motile bacteria following and responding to a moving point source (Barbara and Mitchell, 2003a). Using dark field microscopy, they viewed and measured bacterial isolates capable of tracking free-swimming algal cells. Results showed bacteria following algae in a non-random manner: tracking algae by accelerating, increasing turn frequency, and executing a high number of consecutive turns towards algae. Locsei et al. suggest the bacterial interaction with the algal cells velocity, vorticity and strain rate fields make it capable of tracking the algal cell. This tracking of a source of nutrients suggest an increased availability of nutrients to microbes with a chemotactic ability (Locsei and Pedley, 2009).

There is a recent effort to quantitatively evaluate the growth advantage due to marine chemotaxis in an environment of rapidly dissipating nutrients. The study of environmen-

tally realistic nutrient patch evolution has been hard to execute due to technical limitations to create the right nutrient patch dimensions and dynamics. With new protocols, micro-scale observations have been made possible. Stocker et al. (2008) designed and used microfluidic devices to create patches with environmentally realistic dimensions and dynamics. Using *Pseudoalteromonas haloplanktis*, they observed the formation of bacterial hotspots within tens of seconds in response to a nutrient patch, experiencing a four-fold higher nutrient exposure compared to non-motile bacteria. The chemotactic response was >10 times faster than the classic chemotaxis model for enteric bacteria, resulting in a two-fold nutrient exposure. These results suggest that the chemotactic strategies exerted by microbes influence the carbon turnover rates through the quick formation and dispersion of hot spots, zones of high bacterial productivity (Stocker et al., 2008).

1.5 Summary

A patchy environment with nutrient-rich hot spots may allow for higher productivity if bacteria can access these inhomogeneities within a microenvironment, for which a majority is formed by algal cells. Motility may allow cells to reach nutrients in the phycosphere before they diffuse and chemotaxis provides the ability to recognize and respond to a nutrient gradient produced around an algal cell. Algae serve as an important source of nutrients by producing an abundance of organic carbon. The relationship between algae and bacteria may be crucial in providing organic carbon and other nutrients to the marine food web.

Behavioral and metabolic responses of bacteria to organic matter at the micro-scale directly influence ocean basin-scale carbon fluxes (Azam, 1998). There remain discrepancies in our current knowledge of bacterial nutrient uptake rate and measured carbon turnover for total marine bacteria. It is important to gather quantitative information from

the micro-scale interactions between chemotactic bacteria and nutrient patches including the need to quantify the growth advantage related to motility and the high-energy cost of swimming, to determine the algorithm used by bacteria to decide on reversal frequencies and run lengths. Once a local impact can be identified, it may be possible to scale up to make useful predictions of how marine ecosystems might respond to environmental change.

1.6 Thesis Goals

This thesis aims to determine if clustering around live algal cells can be observed in real-time in a nutrient heterogeneous environment. This goal is achieved through the creation of a protocol that meets all conditions necessary to visualize bacterial clustering. Past models of bacterial clustering vary with some models predicting clustering (Barbara and Mitchell, 2003a; Blackburn et al., 1998; Bowen et al., 1993) while others do not (Jackson, 1989b; Krembs et al., 1998; MullerNiklas et al., 1996).

Bacterial clustering may only exist when a number of conditions are met to mimic the scale of nutrient inhomogeneities in the ocean. Conditions include: (1) a nutrient poor environment with algal cells representing nutrient point-sources, and (2) bacteria that are motile and chemotactic to the algae.

An experimental approach is used where a nutrient poor environment is created through an algal washing technique leaving algal cells to produce nutrient patches. Bacteria that are motile and chemotactic are then introduced and the interactions are observed with a microscope and captured with a camera. This study seeks to identify micro-scale interactions that supports the importance of aquatic microenvironments and their impact on carbon fluxes in the ocean.

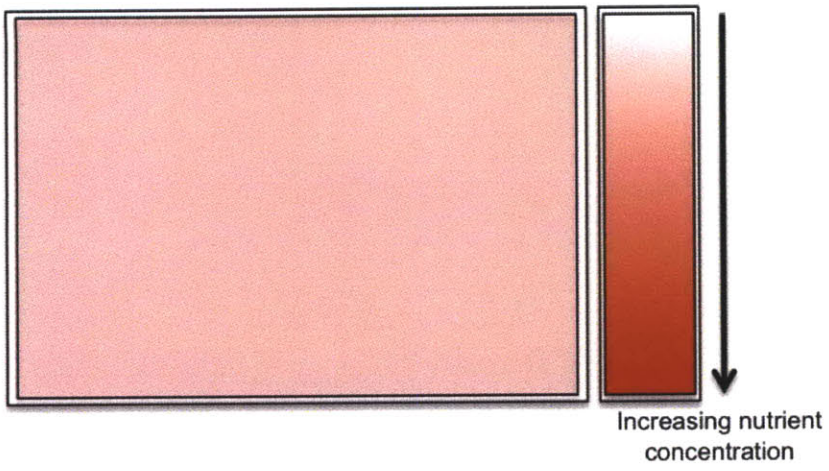

(a)

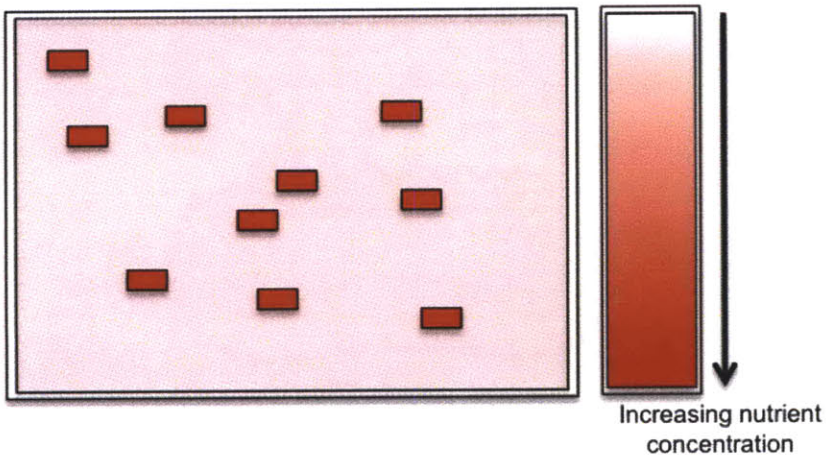

(b)

Figure 1.1: Illustration of (a) homogeneous and (b) heterogeneous nutrient concentration spatial profile of the pelagic zone. (a) Homogeneous profile results in a low bulk concentration throughout the open-ocean. (b) Heterogeneous profile defined by microaggregates (represented as the dark red rectangles) described as having high levels of nutrients, biomass, and productivity. Nutrient concentration scale is provided to the right of each figure.

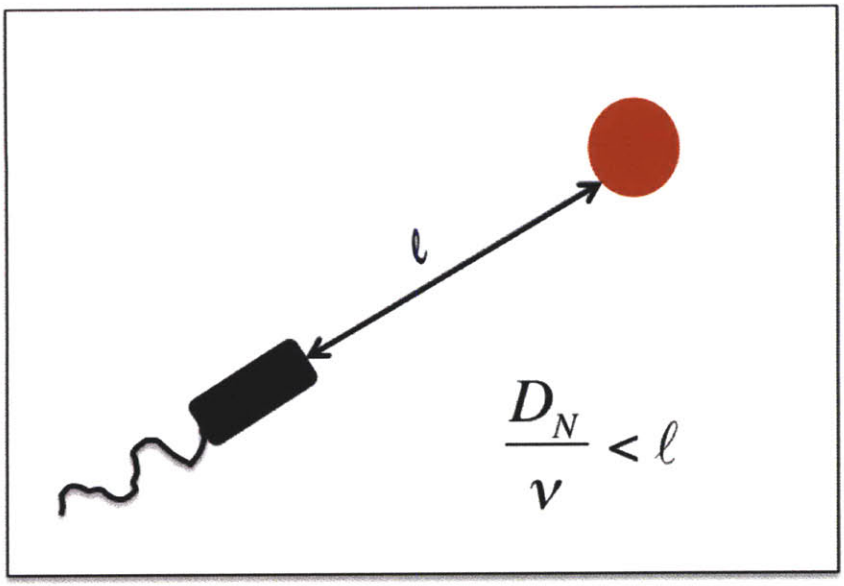

Figure 1.2: Illustration comparing swimming speeds, v, to diffusion, D_N . If a cell were able to swim distance l faster than it takes for the nutrient source to be affected by diffusion, the cell would be in a position to benefit from the ephemeral nutrient hot spot.

2 Materials and Methods

2.1 Model System

For the chemotaxis experiments, a model system consisting of *Pseudoalteromonas haloplanktis* (ATCC700530), a motile heterotrophic bacterium, and *Thalassiosira weissflogii* (CCMP 1051), a non-motile alga, were chosen based on prior observations of positive chemotaxis (Seymour, personal communication). Seymour and coworkers used several combinations of motile bacteria and algal exudates, including *P. haloplanktis* and exudates from *T. weissflogii*, to execute a real-time assessment of the occurrence and strength of chemotaxis and a quantitative analysis of single-cell chemotactic behavior by tracking trajectories of individual microbes. When observing *P. haloplanktis* interaction with a band of algal exudates from *T. weissflogii*, intense aggregation occurred within the chemoattractant band within less than a minute (Figure 2.1a). When comparing bacterial clustering around exudate bands from different algal strains, clustering around exudates from *T. weissflogii* exhibited the second highest strength of accumulation (measured by relative bacteria concentration along the width of the band). (Seymour et al., 2008) (Figure 2.1b).

2.2 Culture Strains and Conditions

Phytoplankton cultures of *Thalassiosira weissflogii* (CCMP 1051) and *Thalassiosira rotula* (CCMP 1647) were obtained from the Provasoli Guillard Center for Culture of Marine Phytoplankton (West Boothbay Harbor, Maine).

Axenic cultures were grown to early to mid-exponential phase in sterile f/2 media (NaCl [400mM], $CaCl_2 \cdot 2\,H_2O$ [10mM], KBr [1.7mM], KCl [10mM], $MgCl_2 \cdot 6\,H_2O$ [20mM], $MgSO_4$ [20mM], H_3BO_3 [0.2mM], $NaNO_3$ [0.882mM], NaH_2PO_4 [0.0362mM], $Na_2SiO_3 \cdot 9\,H_2O$ [0.106mM], $FeCl_3 \cdot 6\,H_2O$ [11.7μM], $Na_2EDTA \cdot 2\,H_2O$ [11.7μM], $CuSO_4 \cdot 5\,H_2O$ [0.0393μM],

$Na_2MoO_4 \cdot 2\,H_2O$ [0.0260μM], $ZnSO_4 \cdot 7\,H_2O$ [0.0765μM], $CoCl_2 \cdot 6\,H_2O$ [0.0420μM], $MnCl_2 \cdot 4\,H_2O$ [0.910μM], vitamin B_1 [0.296μM], vitamin H [2.05nM], vitamin B_{12} [0.369nM]) (Guillard and Ryther, 1962). Cultures were grown in low light conditions for 24 hours/day for 10-20 days reaching densities between $4 \times 10^5 - 2 \times 10^6$ cells/mL.

The marine bacterial isolate *Pseudoalteromonas haloplanktis* (ATCC 700530) was grown to mid-exponential phase, at room temperature, while agitated on a shaker at 200-250 rpm. *P. haloplanktis* was grown in 1% Tryptic Soy Broth (TSB; Difco) supplemented with NaCl at a concentration of 400mM. Cultures were then diluted in 1:20 in an artificial seawater solution (NaCl [400mM], $CaCl_2 \cdot 2\,H_2O$ [10mM], KBr [1.7mM], KCl [10mM], $MgCl_2 \cdot 6\,H_2O$ [20mM], $MgSO_4$ [20mM]), before being starved at room temperature in a wide-mouth flask for 24-72 hours (see Seymour et al., 2008). Final concentration of *P. haloplanktis* were between $3.2 \times 10^8 - 1 \times 10^9$ (Figures 2.2).

2.3 Removal of DOC from Algal Cultures

An algal washing device was designed and fabricated for the purpose of removing the media enriched with dissolved organic carbon (DOC) resulting from the growth of algae in a closed system (25-ml glass culture tubes), while maintaining enough live algal cells to carry out the chemotaxis experiments (Micaela Parker, personal communication). This was done to ensure that nutrient hot spots around algae would form above the background concentration of algal exudates that had accumulated over long periods of growth.

A Nylon mesh filter with a 5 μm pore size (Nitex) was placed over one of two openings of a clear PVC pipe with a 5 cm inner diameter and a height of $\sim$17 cm. The mesh filter was secured by two silicone O-rings with an inner diameter equivalent to the outer diameter of the PVC pipe. The final product (Figure 2.3) allows for filtration while maintaining a live culture, which cannot be obtained by using membrane filters.

All parts of the washer were autoclaved prior to use to minimize risk of contamination and filtration was performed under a UV laminar hood. The washer was fixed above a wide diameter crystalline dish. 50 ml of algal culture at early to mid exponential phase was poured into the opening of the washer and gravity filtration was used to allow for the majority of the liquid to pass through the filter. The majority of the dissolved content passed through the media through the filter in 60 minutes. The algal culture was then diluted with ASW f/2 void of DOM and again the liquid media was allowed to pass through the filter.

The remaining algal culture in the washer was re-suspended with 50 mL of ASW f/2 void of DOM to re-supply the minerals and vitamins needed to continue growth. Because a perfect seal was not created between the PVC pipe and the nylon mesh, the mesh was removed and placed into a new crystalline dish with a known amount of fresh media. The mesh was gently agitated to release algal cells.

DOC concentrations of the culture filtrate were assessed before and after the washing to ensure removal of the majority of organic carbon. Filtrates were obtained by filtration through sterile 0.2 μm membrane filters (Millipore). The concentration of DOC in the culture filtrates was obtained by acidifying with phosphoric acid to pH between 1 and 3 and bubbling with compressed air to remove inorganic carbon. Three to six repeat measurements were taken by a Shimadzu TOC-5000 total carbon analyzer.

Through the use of a hemocytometer, algal counts provide the concentration of algae before and after washing.

2.4 Experimental Setup and Procedure for Chemotaxis Studies

Within hours of algal cultures being washed, algae were combined with *P. haloplanktis*, which were starved in ASW f/2 for >48 hours, into a deep-well microscope slide, which

can contain a volume of 85 μl. A cover slide was placed on top of the deep well to create a seal. An inverted microscope (Eclipse TE2000ϵ, Nikon) and CCD camera (PCO1600, Cooke) were used to visualize and record the interactions. The slide was placed on the stage of the inverted microscope within <10 seconds of the addition of algae and bacteria.

2.5 Data Acquisition and Processing

Direct observations were conducted using the inverted microscope with a 20X objective. Positions and swimming paths of individual cells were recorded at 2 min intervals for 8-30 min, by recording sequences of 320 frames at 32 frames per second. The cameras field of view was 1600 x 1200 pixel (0.9mm x 1.2mm).

Chemotaxis to algal cells was assessed by qualitatively comparing bacterial swimming tracks in the presence and absence of algae. Accumulation of bacteria around single algae was immediately apparent, due to the intense clustering of trajectories. Image analysis software (IPLab) was used to visualize this, by first subtracting consecutive frames from one another and then stacking all frames within one sequence (Figure 2.4). The resulting picture captures motile cells only, effectively removing any non-moving objects.

The locations of algal cells were identified through direct observation of the images.

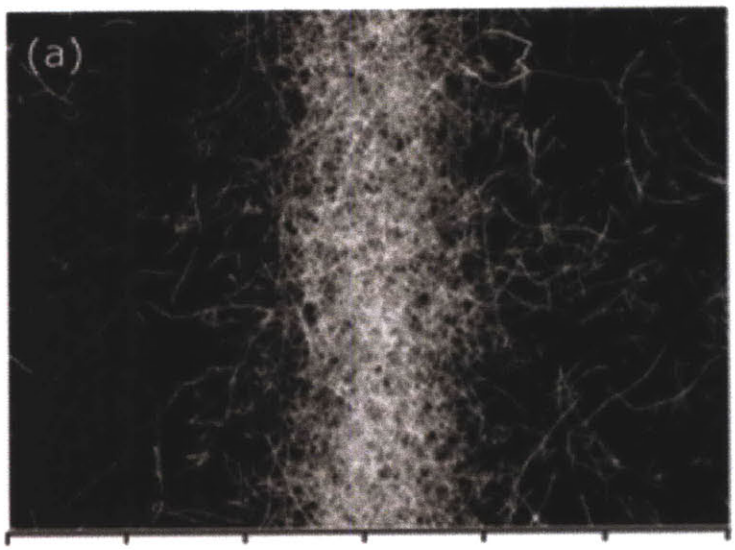

(a)

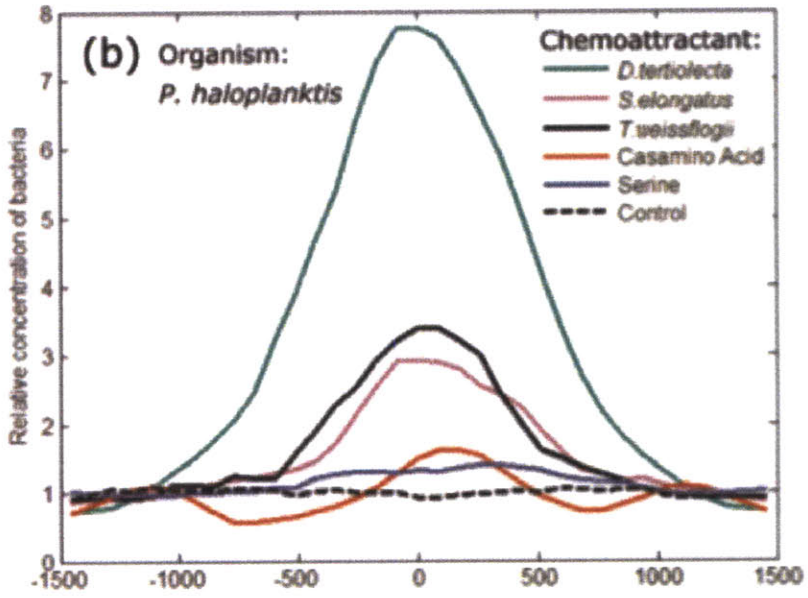

(b)

Figure 2.1: (a) Intense aggregation of *P. haloplanktis* around the *T. weissflogii* algal exudate chemoattractant band within less than a minute. (b) Algal exudates from *T. weissflogii* also exhibited a large attraction(black solid line) of bacteria out of the array of algal strains tested. (Figures courtesy of Seymour) (Seymour, 2008)

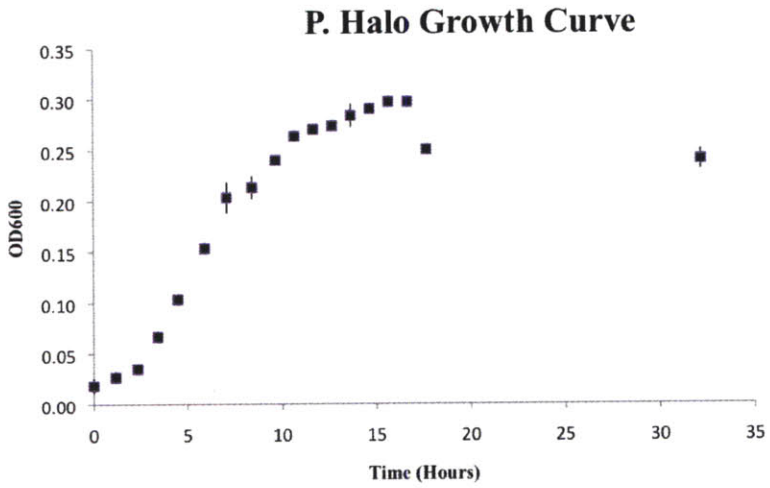

(a)

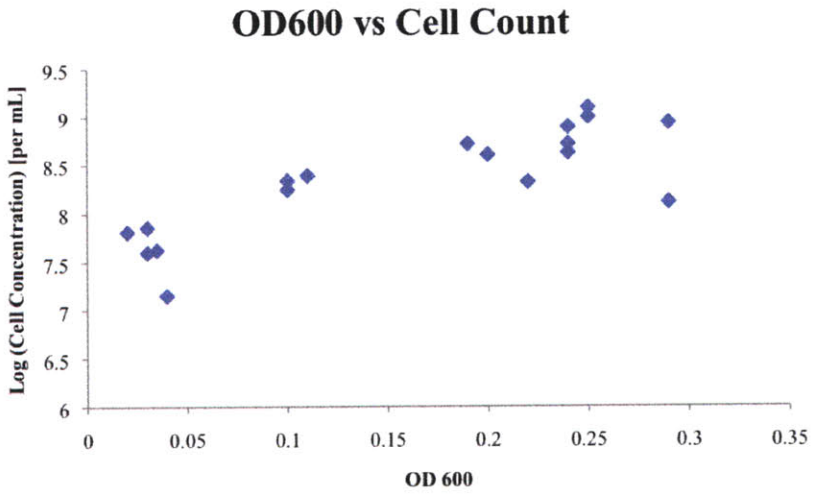

(b)

Figure 2.2: (a) Growth curve of starved *P. haloplanktis* (ATCC700530). Strain is first grown overnight in 1% Tryptic Soy Broth (TSB) and then diluted in 1:20 Artificial Seawater (ASW) f/2 media. Growth curve at time = 0 hours represents the optical density immediately following dilution. Measurements were taken from three samples. Standard deviation bars are usually too short to be visible. (b) To determine cell concentration from OD measurements, cell counts were taken at varying time points for three samples. Results in a *P. haloplanktis* concentration of $3.2 \times 10^8 - 1 \times 10^9$ after 24 hours of starvation.

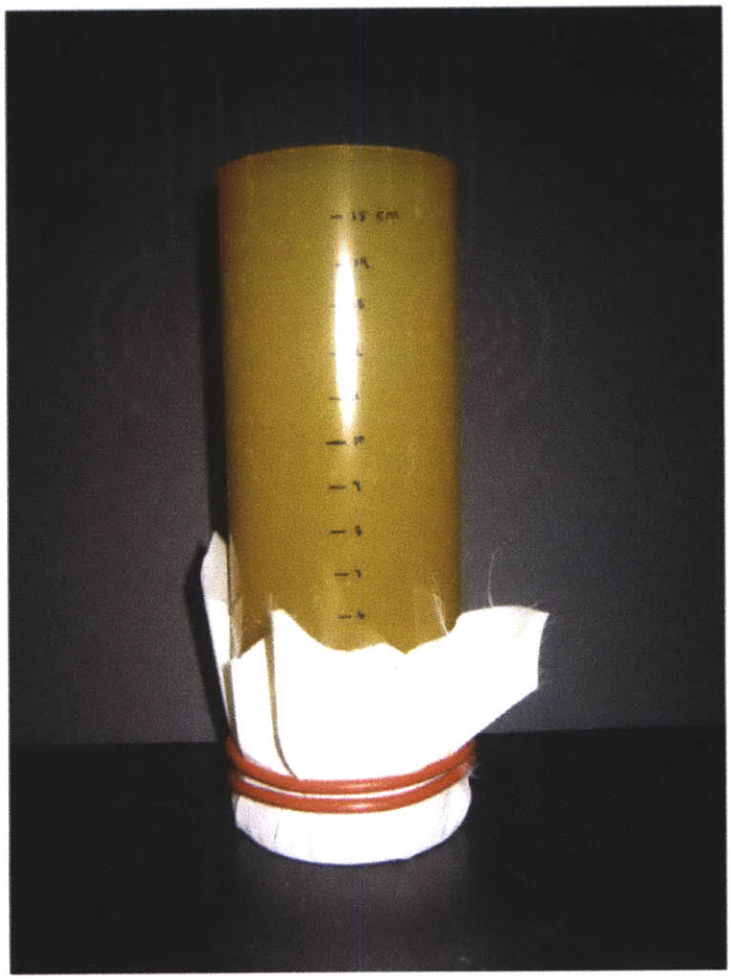

Figure 2.3: Photo of the algal washer instrument. A PVC pipe with a 5 cm inner diameter is covered on one end by a nylon mesh filter (with a 5-μm pore size). This mesh filter is secured by 2 silicon O-rings. All materials are autoclavable to ensure sterile equipment and decrease risk of contamination of algal cultures. Gravity filtration is used to allow dissolved organic carbon (DOC) to leave algal cultures.

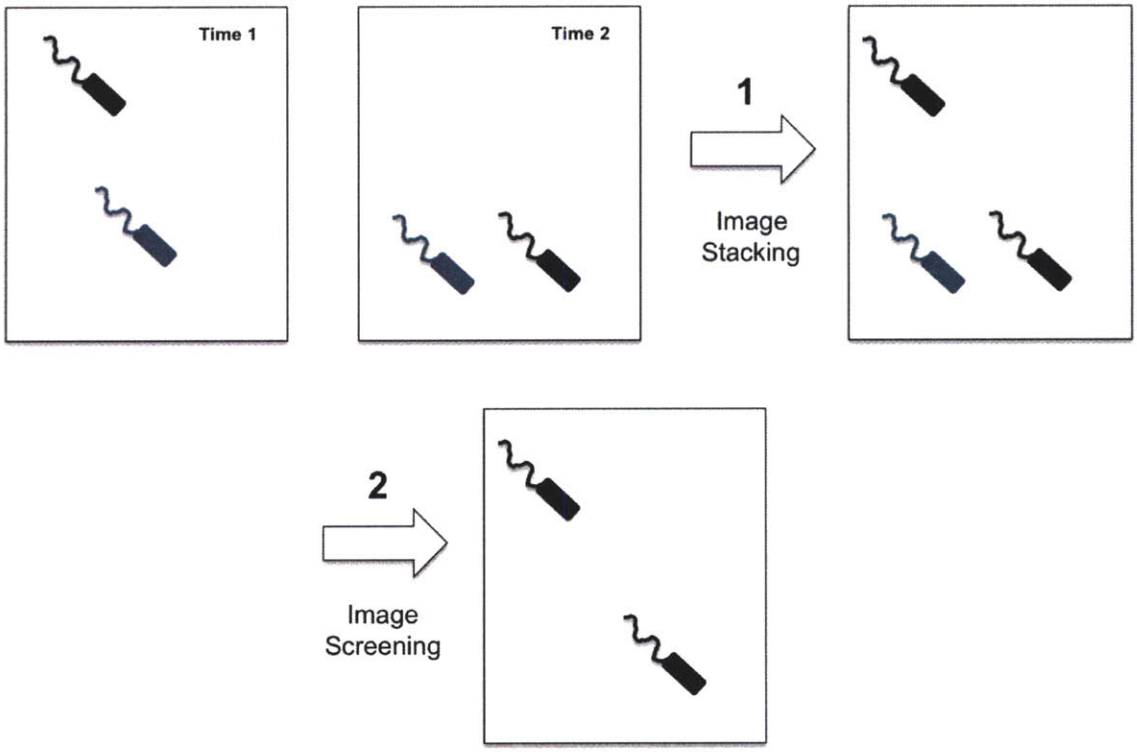

(a)

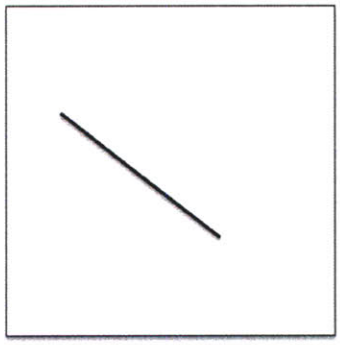

(b)

Figure 2.4: (a) Illustration of the image processing needed to analyze bacterial interaction with algae captured with inverted microscope (Eclipse TE2000ϵ, Nikon) and CCD camera (PCO1600, Cooke). In the first step, image stacking, all frames were combined into one frame. Step 2, image screening, removed all non-moving objects in the combined frame. (b) Illustration of a bacterial track representing a single bacterial cell and its movement throughout a frame sequence.

3 Results and Discussion

3.1 Assessment of Algal Washer

Flow of *Thalassiosira weissflogii* cultures through the algal washer was characterized to determine if the DOC removal protocol timescale fit within the scope of the chemotaxis experiments. The hydraulic conductivity of the mesh filter and the clogging caused by algal cells were calculated to determine the amount of time required for adequate filtration. Algal and DOC concentrations were determined post filtration to assess whether minimum concentrations of cells were present and the majority of dissolved exudates had passed through.

3.1.1 Flow Properties

Darcys Law

$$Q = KA\frac{dh}{dl}$$

was used to describe flow through the Nylon mesh filter, where

Q, flow rate[cm ^{3}/s]
K,swimming speed[cm ^{2}/s]
A, cross-sectional area of flow[cm ^{2}]
dh, pressure head
dl, thickness of filter [cm]

Due to the setup of the algal washer (Figure 3.1), pressure at the exit of the washer (P_A) is

$$P_A = 0$$

When plugged into the pressure head equation,

$$dh = P_B - P_A = P_B = h$$

where h is the height of the water column in the algal washer.

Through several flow experiments using only f/2 media, the hydraulic conductivity (K) of the mesh filter was determined. By plotting $A\frac{dh}{dl}$vs. $-Q$ (Figure 3.2), the slope of the linear best fit describes the hydraulic conductivity, K (Table 3.1).

Once the nutrient media passed through the mesh filter, the effective area, A, was decreased due to the silica precipitates in the f/2 media. To determine the loss of cross-sectional area of flow, 300 ml of ASW f/2 media was passed through the filter twice, and an effective area was calculated by comparing the two flows. The effective area was decreased by approximately 50%. Hydraulic conductivity was re-calculated using the adjusted area.

The average hydraulic conductivity of the filter was calculated to be 7.7×10^{-5}cm ^{2}/s (standard deviation: 1.01×10^{-5}cm ^{2}/s). Using relative permeabilities, the mesh filter provides a semi-pervious environment to the likes of very fine sand (Bear, 1988).

When algal cultures were passed through the algal washer, an additional clogging factor needed to be taken into account, caused by the settling of algal cells which resulted in the decrease of filter cross-sectional area over time. The adjusted Darcys equation is

$$Q' = CKA\frac{dh}{dl}$$

or

$$Q' = K'A\frac{dh}{dl}$$

where C is the dimensionless factor that describes the clogging effect and $K' = CK$. By plotting $A\frac{dh}{dl}$vs. $-Q$ (Figure 3.3), the slope of the linear best fit describes the hydraulic conductivity, K' (Table 3.2). The average K was calculated to be 6.35×10^{-7}cm ^{2}/s (standard deviation: 5.00×10^{-8}cm ^{2}/s). Thus, the clogging factor was calculated to be $C = 10^{-2}$ Using the calculated C and K values, the amount of time needed to allow 20-30 ml of dissolved content from a 50 ml sample of filtrate to pass through the filter was calculated to be between 55 and 100 minutes (Table 3.3). Not all of the 50 ml of the sample passed through the filter due to the volume occupied by algal cells.

3.1.2 Assessing Algal Loss and DOC Dilution Rates

The washing technique introduced some loss of algae. Due to the range of cell sizes in an algal culture, a certain number of cells may pass through the 5 μm filter or possibly remain stuck in the filter even after agitation. There may be cells that burst due to pressure and shear forces caused by the washing technique. For *T. weissflogii*, there was a 60% loss from the original cell concentration, for early and mid exponential phase cultures.

To estimate DOC values in post-washed algal cultures, a DOC conversion number [mgC/cell] was measured to evaluate the dissolved content that remains in the algal washer. A DOC conversion number was obtained through division of the net DOC (calculated as DOC in ASW f/2 media subtracted from the DOC in the sample) of sample filtrates by the algal count in the same sample. The majority of the net DOC in the post-washed algal culture is assumed to be from dissolved content that had not passed through the filter. Wetting by adhesion forces to algal cells, cohesion, and the very low flow rates as the pressure head decreases most probably cause the remaining dissolved organic carbon.

Net DOC per cell was calculated to be between $1.5 \times 10^{-9} - 3.3 \times 10^{-9}$ mgC/cell for *T. weissflogii*. Multiplication by the average cell concentration (post-washing) provides DOC

concentrations in final sample. For *T. weissflogii*, dilution rates are between $\frac{1}{3} - \frac{1}{6}$. The range of dilution rates is likely due to variability in cell concentration, filtration protocol, and output data from the TOC analyzer.

Prior to microscopic observations, algal concentrations were again diluted. Two dilution settings were used: 1:7 and 1:16, for a final dilution rate ranging from 1:20 to 1:100.

3.2 Chemotaxis Experiments

No accumulation around *T. weissflogii* cells was observed in any of the 16 samples tested. Bacteria and algal concentrations varied among samples. *P. haloplanktis* cell concentrations ranged between $4 \times 10^7 - 1 \times 10^9$ cells/ml and algal cell concentrations varied between $6.4 \times 10^3 - 1.6 \times 10^5$ (Table 3.4). The ratio of *T. weissflogii* to *P. haloplanktis* varied from 1:250 to 1:50000.

Several explanations could describe the lack of clustering observed (Figure 3.4). *P. haloplanktis* may not be chemotactic to live *T. weissflogii* even though chemotaxis to the algal exudates (from spent media) was observed in prior experiments (Seymour et al., 2008). *T. weissflogii* could be exuding microbial toxins in the presence of bacteria that could prevent bacteria from clustering. But, negative chemotaxis was not observed and would most likely occur if toxins were being produced. No difference in bacterial behavior was observed when compared to control samples (no algae).

T.weissflogii may not exude photosynthetic products while under the microscope if there were illumination limitations. Illumination under the microscope was measured with a Scalar PAR Irradiance Sensor (Biospherical Instruments, QSL-2100) and compared to illumination conditions during cultivation. Illumination under the microscope ranged from 92-135 μE/m ^{2}s, depending upon the light intensity used. Illumination during cultivation ranged from 20-35 μE/m ^{2}s. A published study found the upper range of acceptable

illumination for *T. weissflogii* growth during high light conditions to be 300 μE/m ^{2}s (Parker and Armbrust, 2005). This suggests that illumination was not the reason for the lack of accumulation.

Another possible cause for the lack of clustering might have been the small size of the nutrient hot spot created by each algal cell (Figure 3.5). The bacteria may swim through the phycosphere too quickly to sense a change in concentration. To further investigate cell-size dependence for bacterial clustering, chemotaxis experiments were repeated for a larger alga from the same genus (Table 3.5), *Thalassiosira rotula* (CCMP 1647). The experimental protocol was identical for *T. rotula* as for *T. weissflogii.*

The clogging factor calculated for *T. weissflogii* was also used to determine the total time required for the filtration of exudate-enriched media from *T. rotula.* This clogging factor was assumed to be a conservative value and proved to be more than the minimum amount of time to allow for the majority of dissolved content to pass through.

Though *T. rotula* is known to form chains using silica spindles, no chains were observed during microscopic observations. There may have been chain breakage during the algal washing.

This time, chemotaxis experiments revealed strong accumulation around individual algal cells. Bacterial clustering was observed in 3 of the 4 samples (Table 3.6). Within <30 s, the number of tracks near the algal cell increased significantly, resulting in bacterial clustering around algal cells (Figures 3.6 and 3.7). Over time the concentration of tracks decreased. Bacterial clustering was sustained for several minutes. It is not entirely clear why accumulation decreased over time. Potential reasons include (1) light stress, (2) stress from slide heating, and (3) cell lysis. Dissipation of tracks occurred at different rates among different samples. If dissipation is correlated to an imbalance between nutrient production and nutrient utilization, varying dissipation rates may be due to the variability in algal size.

Comparison of Figure 3.6e to 3.7f results in the identification of a larger alga in Figure 3.7. The larger alga (Figure 3.7) elicited a longer accumulation period, the accumulation lasting at least 4 minutes, than the smaller alga (Figure 3.6), where the accumulation lasted at least 2 minutes.

This paper represents supporting evidence of clustering around phytoplankton and, importantly, suggests a size-dependence of the algae in attracting bacteria. This study suggests that bacteria may cluster around algal cells, and potentially other small nutrient-enriched patches in the ocean, which could increase nutrient uptake rates of the bacteria that can exploit these hot spots.

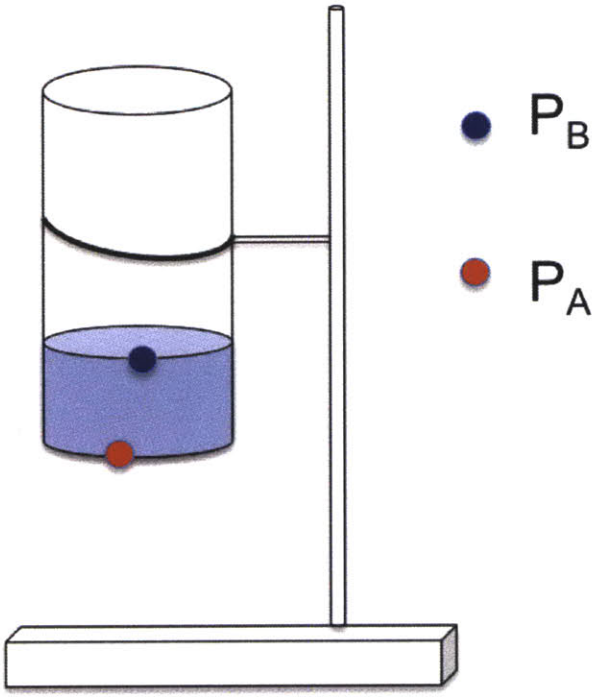

Figure 3.1: Illustration of the algal washer setup. P_A and P_B equal pressure at respective points.

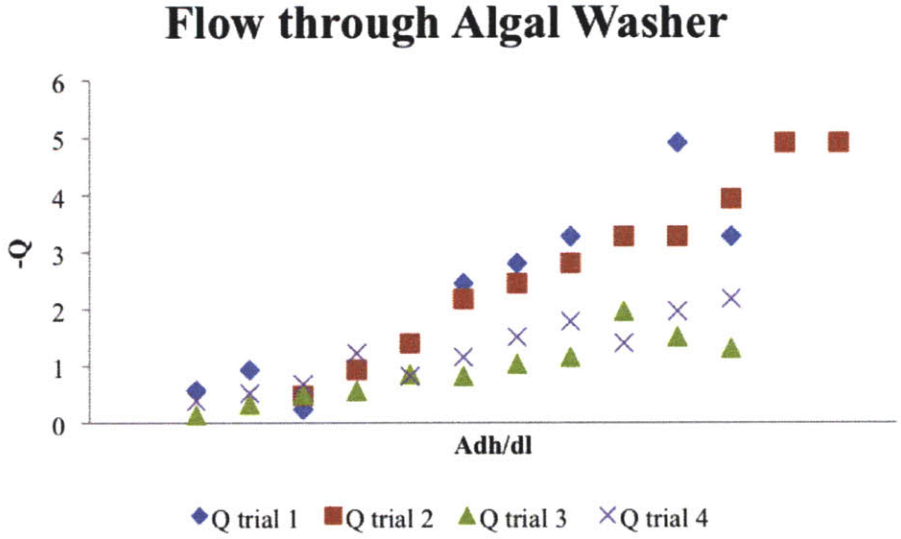

Figure 3.2: 300 mL of ASW f/2 media was passed through the filter to quantify flow rate, $Q[\text{cm}^3/\text{s}]$ and hydraulic conductivity, $K[\text{cm}^2/\text{s}]$. Darcy's Law, $Q = KA\frac{dh}{dl}$, was used to evaluate K. Q was plotted against $A\frac{dh}{dl}$. Slope of regression curve equals K. Measurements were taken from 4 trials.

Table 3.1: Hydraulic Conductivity of Nylon Mesh Filter

	Slope - K	$R^{2\ d}$	Standard Error^e
Trial 1^a	7.35×10^{-5}	0.92	0.66
Trial 2^a	8.33×10^{-5}	0.99	0.22
Trial 3^b	4.33×10^{-5}	0.82	0.24
Trial 4^b	3.21×10^{-5}	0.95	0.20
Trial 3^c (0.5A)	8.65×10^{-5}		
Trial 4^c (0.5A)	6.43×10^{-5}		

a - Flow experiment began with a dry filter.

b - Flow experiment began with a wet filter. Wetting occurred by passing 300 mL of ASW f/2 through instrument.

c - Hydraulic conductivity values were evaluated assuming area of filter decreased by 50%.

d - Statistical measure of how well the regression data approximated real data points.

e - Measure of the predictive error of Q from regression data compared to actual values.

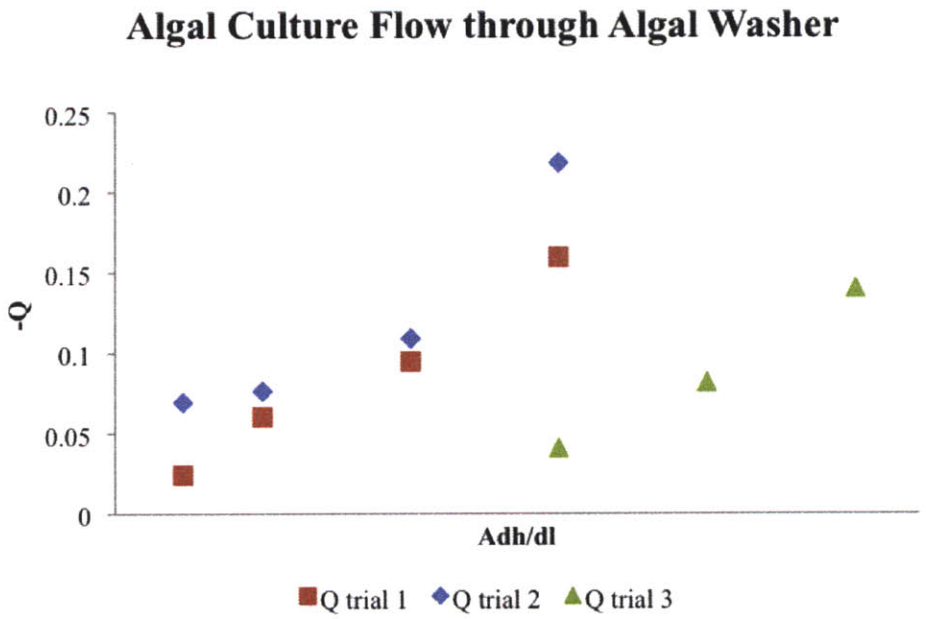

Figure 3.3: Algal cultures were passed through filter to quantify the clogging factor, C, in the adjusted Darcy's Law equation, $Q' = K'A\frac{dh}{dl}$ where $K' = CK$. Slope of regression curve equals K'. Measurements were taken from three trials.

Table 3.2: Adjusted Hydraulic Conductivity of Nylon Mesh Filter, K'

	Slope - K'	$R^{2\ b}$	Standard Error^c
Trial 1^a	6.14×10^{-7}	0.99	0.01
Trial 2^a	6.92×10^{-7}	0.94	0.03
Trial 3^a	5.99×10^{-7}	0.99	0.01

a - Flow experiment began with a dry filter.
b - Statistical measure of how well the regression data approximated real data points.
c - Measure of the predictive error of Q from regression data compared to actual values.

Height [cm]	Volume Remaining [mL]	Q [cm^3/s]	Total Time [min]
2.55	50	8.58×10^{-3}	0
2.05	40.18	6.90×10^{-3}	23.72
1.55	30.37	5.21×10^{-3}	55.11
1.05	20.55	3.53×10^{-3}	101.49
0.55	10.73	1.84×10^{-3}	190.32
0.05	0.91	1.57×10^{-4}	1234.67

Table 3.3: Calculation of the time needed to filter algal samples before chemotaxis experiment. Starting volume is 50 mL and height was approximated using the cylinder volume equation. Adjusted Darcys Law is used to solve for Q, using calculated Clogging Factor, $C = 10^{-2}$; and calculated hydraulic conductivity, $K = 7.60 \times 10^{-5}[cm^2/s]$

Table 3.4: Detailed Conditions of Chemotaxis Experiments with *T. weissflogii* and *P. haloplanktis*

ID	Concentration of *P. haloplanktis* [cells/mL]	Concentration of *T. weissflogii* [cells/mL]	Chemotaxis Observed
A1	$9.5 \times 10^7 - 3.0 \times 10^8$	6.4×10^3	No
A2	$2.0 \times 10^8 - 6.3 \times 10^8$	7.5×10^4	No
A3	$2.4 \times 10^8 - 7.5 \times 10^8$	6.0×10^4	No
A4	$4.0 \times 10^7 - 1.3 \times 10^8$	1.6×10^5	No
A5	$2.8 \times 10^8 - 8.8 \times 10^8$	2.5×10^4	No
B1	$1.2 \times 10^8 - 3.8 \times 10^8$	7.6×10^4	No
B2	$1.2 \times 10^8 - 3.8 \times 10^8$	7.6×10^4	No
B3	$2.8 \times 10^8 - 8.8 \times 10^8$	7.1×10^4	No
B4	$2.4 \times 10^8 - 7.6 \times 10^8$	3.6×10^4	No
C1	$3.2 \times 10^8 - 1.0 \times 10^9$	0	Control
C2	$3.0 \times 10^8 - 9.4 \times 10^8$	4.3×10^4	No
C3	$3.0 \times 10^8 - 9.4 \times 10^8$	4.3×10^4	No
C4	$3.0 \times 10^8 - 9.4 \times 10^8$	1.8×10^4	No
D1	$3.2 \times 10^8 - 1.0 \times 10^9$	0	Control
D2	$3.0 \times 10^8 - 9.4 \times 10^8$	8.5×10^4	No
D3	$3.1 \times 10^8 - 9.8 \times 10^8$	3.4×10^4	No
D4	$3.1 \times 10^8 - 9.8 \times 10^8$	3.4×10^4	No
D5	$3.1 \times 10^8 - 9.8 \times 10^8$	3.4×10^4	No

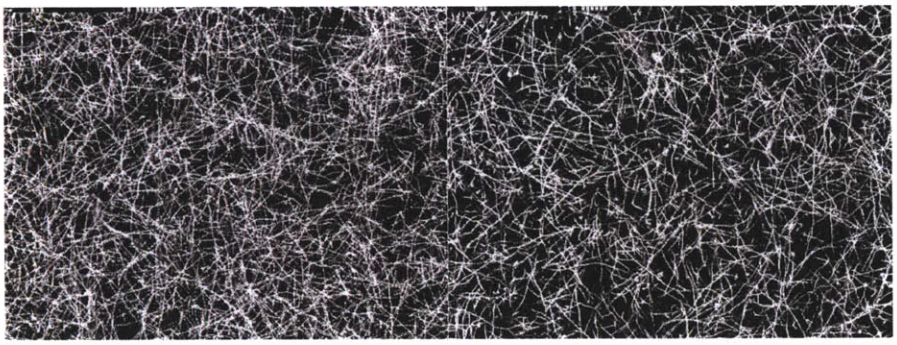

(a) 0 min (b) 6 minutes

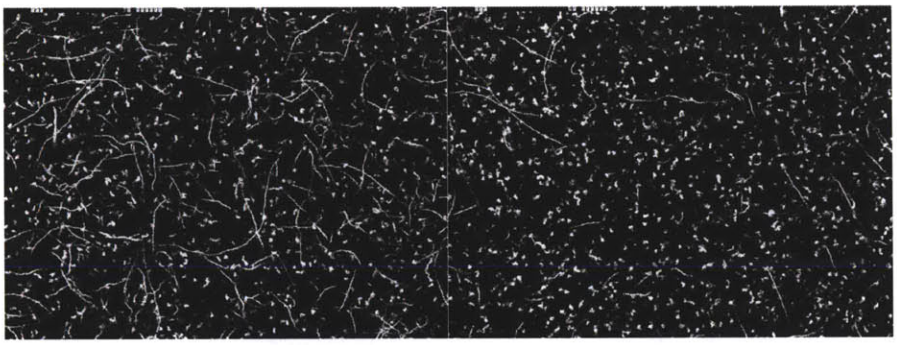

(c) 16 minutes (d) 26 minutes

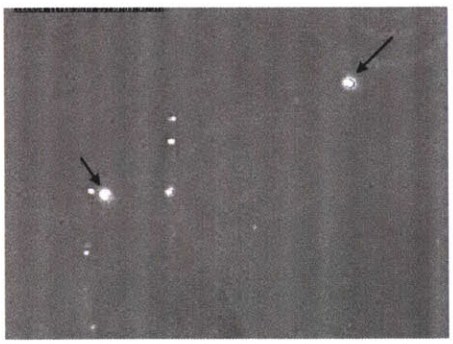

(e) reference

Figure 3.4: Chemotaxis experiment with *P. haloplanktis* and *T. weissflogii*. Figures (a) - (d) are processed images at varying time points (standard deviation of approximately 30 seconds) within one experiment (ID: C3). Figure (e) locates algal cells. No accumulation of tracks around algal cells are observed. Movement measured by observed number of tracks decreases over time which also occurred in control experiments.

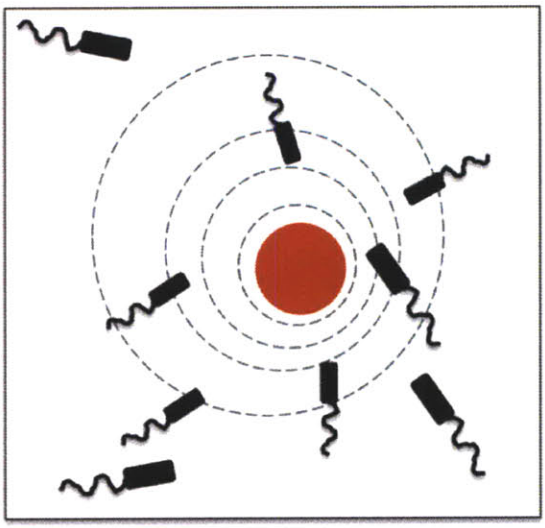

(a)

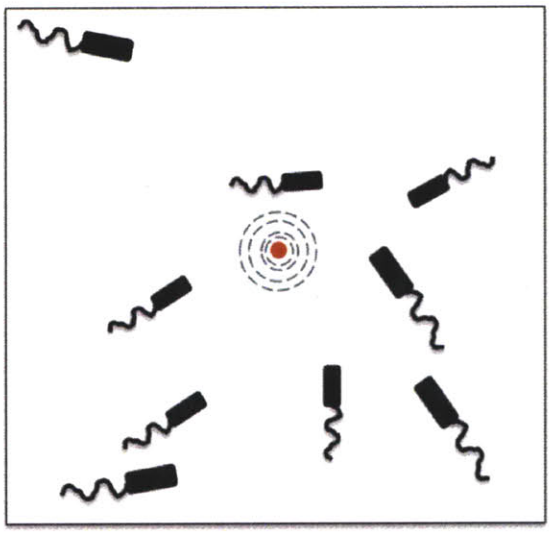

(b)

Figure 3.5: IIllustration of the effect of phycosphere size. (a) When the gradient is larger than the body length of a cell, it can move along the gradient to find a point of desired increase or decrease in concentration. (b) When the gradient produced is less than the body length of the cell, it will not recognize the gradient even if encountering the gradient. The cell would effectively be swimming through the gradient too fast. In this case, a cell would have to rely purely on encounter rates and colliding into an environment that is desired.

Table 3.5: Algae Cell Size for *Thalassiosira* Strains. (Source: Provasoli Guillard Center for Culture of Marine Phytoplankton)

Strain	Cell Length μm	Cell Width μm
Thalassiosira weissflogii	10–20	8–15
Thalassiosira rotula	18–30	16–20

Table 3.6: Detailed Conditions of Chemotaxis Experiments with *T. rotula* and *P. haloplanktis*

ID	Concentration of *P. haloplanktis* [cells/mL]	Concentration of *T. rotula* [cells/mL]	Chemotaxis Observed
E2	$2.0 \times 10^8 - 6.5 \times 10^8$	5.3×10^4	Yes
E3	$2.0 \times 10^8 - 6.5 \times 10^8$	2.6×10^4	Yes
E4	$1.5 \times 10^8 - 4.7 \times 10^8$	2.6×10^4	No
E5	$7.9 \times 10^7 - 2.5 \times 10^8$	2.8×10^4	Yes

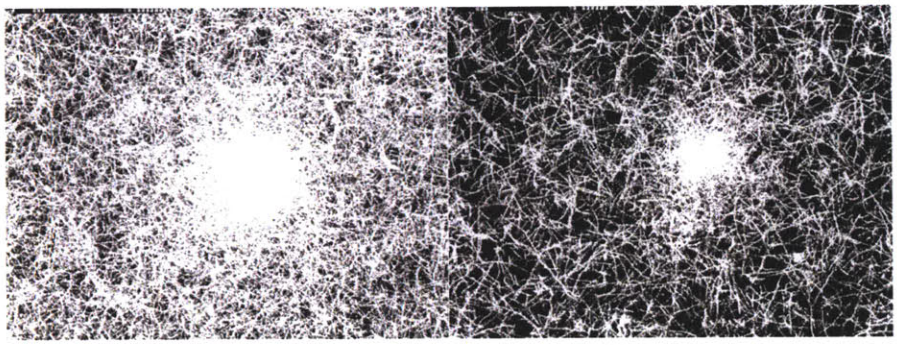

(a) 0 minutes (b) 2minutes

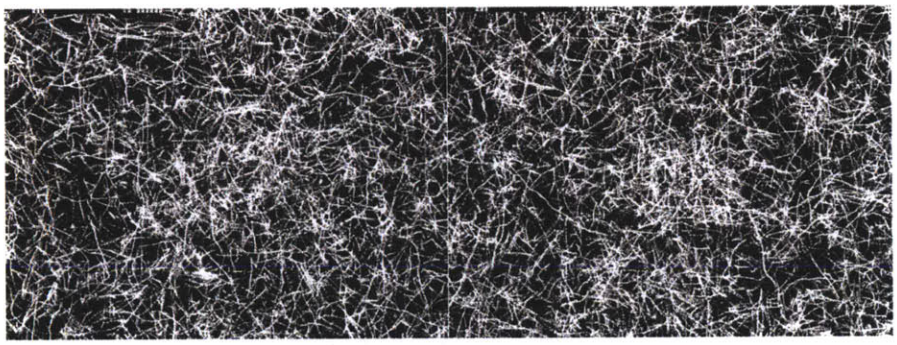

(c) 4 minutes (d) 6 minutes

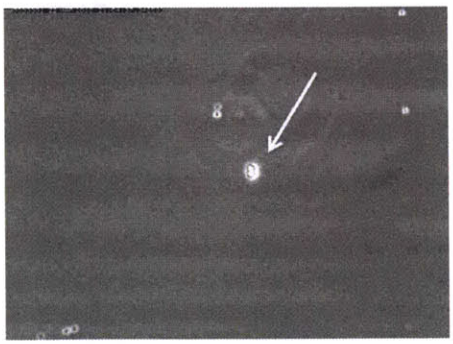

(e) reference

Figure 3.6: Chemotaxis experiment with *P. haloplanktis* and *T. rotula*. Figures (a) - (d) are processed images at varying time points (standard deviation of approximately 30 seconds) within one experiment (ID: E3). Figure (e) locates algal cells. Accumulation of tracks occurs within less than 30 seconds around algal cells are observed and decreases over time.

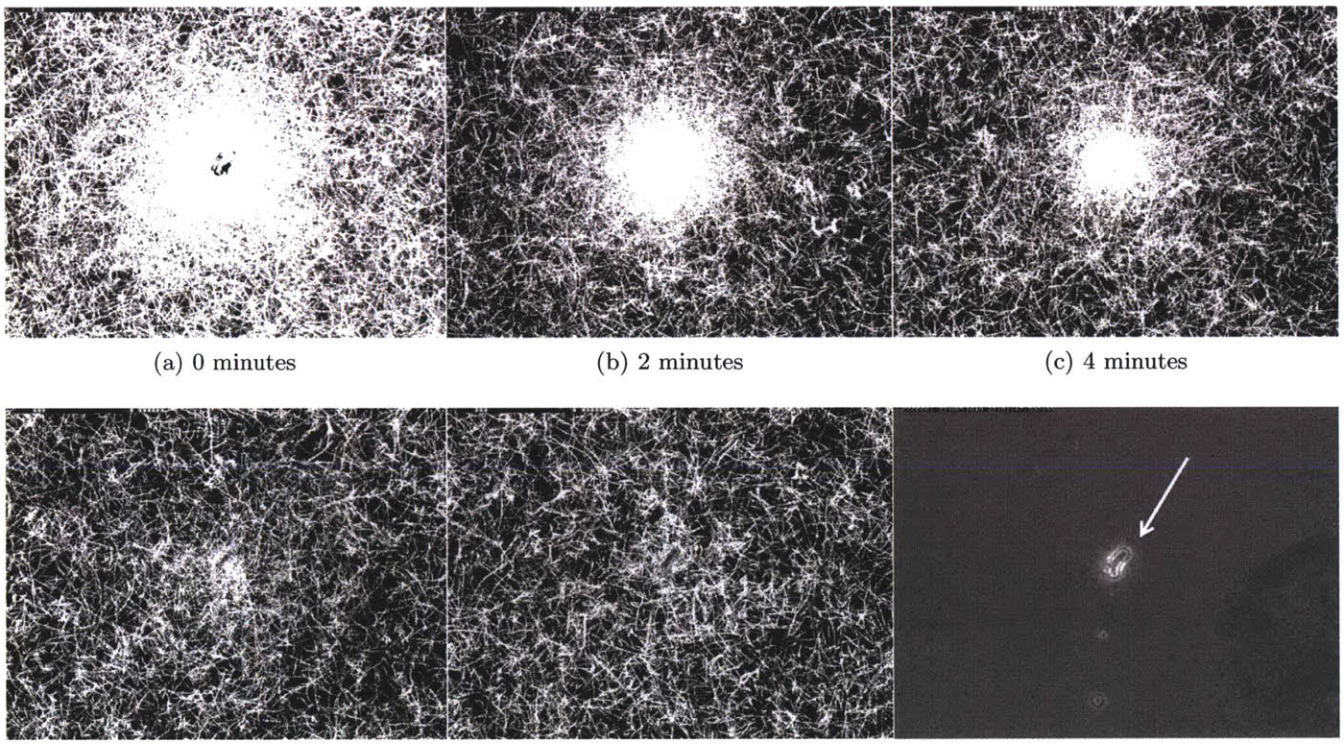

(a) 0 minutes (b) 2 minutes (c) 4 minutes

(d) 8 minutes (e) 10 minutes (f) reference

Figure 3.7: Chemotaxis experiment with *P. haloplanktis* and *T. rotula*. Figures (a) - (d) are processed images at varying time points (standard deviation of approximately 30 seconds) within one experiment (ID: E5). Figure (e) locates algal cells. Accumulation of tracks occurs within less than 30 seconds around algal cells are observed and decreases over time.

4 Conclusion

The growing evidence of microscale heterogeneity for nutrients in the ocean supports the existence of two groups of bacteria: passive and opportunistic bacteria. Passive bacteria efficiently use low bulk nutrient levels, whereas opportunistic bacteria take advantage of nutrient-rich hot spots (Polz et al., 2006). The tight coupling of bacteria and algae in the microbial loop (Azam and Malfatti, 2007) suggest that the microhabitats created by algae may be a large contributor to carbon flux rates between algae and opportunistic bacteria. My thesis explores the importance of this marine microenvironment by observing the response of bacteria in a controlled microenvironment. This topic was approached by asking: Is there micro-scale clustering of bacteria around algal cells?

The first part of my thesis focused on creating one such microenvironment. Creation of the microenvironment with live cells was motivated by earlier laboratory-generated microscale resource patches at environmentally realistic spatiotemporal scales using microfluidic devices (Seymour et al., 2009). By constructing a gravity filter with a nylon mesh screen, it was confirmed experimentally that a nutrient poor environment (low concentration of DOC) could be created with an abundant concentration of live algal cells.

The second part of my thesis focused on using a laboratory-generated heterogeneous environment to observe bacterial responses to algal cells. With the use of a camera and microscope, bacterial clustering was confirmed within thirty seconds between *P. haloplanktis* and *T. rotula*, while clustering was not observed for the smaller alga, *T. weissflogii* . Clustering around live cells also suggests this mechanism may not be limited to massive algal deaths from blooms as concluded by prior experiments (Grossart et al., 2001).

Some details of the relationship still remain unclear: Why was *P. haloplanktis* chemotactic to *T. rotula* but not *T. weissflogii*? Was it due to size as originally hypothesized? Alternatively, *T. rotula* may release nutrients for which bacteria have a larger affinity. Or,

T. weissflogii could be releasing different metabolites at varying growth stages as observed in other algae (Barofsky et al., 2009). Could *P. haloplanktis* exhibit clustering if exposed to *T. weissflogii* at a later or earlier growth phase?

Why does the clustering dissipate over time? Is this phenomenon a result of the experimental procedure or is it a mechanism transferable to the environment? By removing external stresses (e.g. using an infrared filter to minimize slide heating), or varying the ratio of algae:bacteria, observations of the effect on bacterial clustering may increase our knowledge of the cause for the dissipation.

Further work will include the evaluation of the growth rate advantage of motile bacteria by comparing growth in co-cultures with a bacterial wild type and an isogenic motility mutant. Algal cultures will be cultivated to early to mid exponential phase (10-20 days), followed by the introduction of one or both the motile and mutant strain. By defining observed growth over time between single inoculation growths and co-cultured growths, we may be able to observe differences in growth rates. Characterizing growth rates in a co-growth without algae can describe competition between the two strains. Since the two strains are solely differentiated by the ability to be motile, it is very likely the differences observed can be explained by motility. Roseobacter strain Y4I and the motility mutant Y4I1AA7 (Tn-5 transposon insertion in histidine sensor kinase) obtained from Alison Buchan (University of Tennessee, Knoxville) will be used. Roseobacter represents a dominant bacterial group found in the open-ocean. Observation of interactions with phytoplankton may be an important lifestyle in the ocean (Buchan et al., 2005).

Overall, this work advances our understanding of microbial ecology and biogeochemistry in the ocean. Metabolic processes and ecological preferences may vary among microbial communities and lead to a delicate balance between passive and opportunistic bacteria. While only one bacterial strain and alga genus were investigated, these findings depict

a feature that may be common to other microenvironments. Observations of bacterial clustering reveal a fundamental mechanism used by some bacteria to survive in the pelagic environment.

If the overall coupling between bacteria and algae proves to be the rate-limiting step in the biogeochemical cycling of carbon, the determination of the primary types of coupling will be very important to advance the knowledge and quantification of carbon fate and transport and predict how those rates will be affected by change in spatial distribution and concentration of algae (such as increasing the concentration of algae through iron fertilization). Understanding the types and rates of coupling between carbon fixers and carbon users may advance our knowledge of the biogeochemical cycling of carbon. Opportunistic heterotrophs may have a significant impact on the carbon transfer rates in microhabitats that exhibit heterogeneous nutrient profiles.

References

Adler J. Chemoreceptors in Bacteria. Science (1969) 166:1588-&.

Adler J. Chemotaxis in bacteria. Annual Review of Biochemistry (1975) 44:341-356.

Azam F. Microbial control of oceanic carbon flux: The plot thickens. Science (1998) 280:694-696.

Azam F, Fenchel T, Field JG, Gray JS, Meyerreil LA, Thingstad F. The Ecological Role of Water-Column Microbes in the Sea. Mar. Ecol.-Prog. Ser. (1983) 10:257-263.

Azam F, Malfatti F. Microbial structuring of marine ecosystems. Nature Reviews Microbiology (2007) 5:782-791.

Barbara GM, Mitchell JG. Formation of 30- to 40-micrometer-thick laminations by high-speed marine bacteria in microbial mats. Applied and Environmental Microbiology (1996) 62:3985-3990.

Barbara GM, Mitchell JG. Bacterial tracking of motile algae. Fems Microbiology Ecology (2003a) 44:79-87.

Barbara GM, Mitchell JG. Marine bacterial organisation around point-like sources of amino acids. Fems Microbiology Ecology (2003b) 43:99-109.

Barofsky A, Vidoudez C, Pohnert G. Metabolic profiling reveals growth stage variability in diatom exudates. Limnol. Oceanogr. Methods (2009) 7:382-390.

Bear J. Dynamics of fluids in porous media. (1988): Dover Publications.

Bell W, Mitchell R. Chemotactic and Growth Responses of Marine Bacteria to Algal Extracellular Products. Biological Bulletin (1972) 143:265-277.

Berg H. How to track bacteria. Review of Scientific Instruments (1971) 42:868.

Berg HC, Anderson RA. Bacteria Swim by Rotating their Flagellar Filaments. Nature (1973) 245:380-382.

Berg HC, Brown DA. Chemotaxis in Escherichi-Coli Analyzed by 3-Dimensional Tracking. Nature (1972) 239:500.

Blackburn N, Azam F, Hagstrom A. Spatially explicit simulations of a microbial food web. Limnol. Oceanogr. (1997) 42:613-622.

Blackburn N, Fenchel T, Mitchell J. Microscale nutrient patches in planktonic habitats shown by chemotactic bacteria. Science (1998) 282:2254-2256.

Bowen JD, Stolzenbach KD, Chisholm SW. Simulating Bacterial Clustering Around Phytoplankton Cells in a Turbulent Ocean. Limnol. Oceanogr. (1993) 38:36-51.

Buchan A, Gonzalez JM, Moran MA. Overview of the marine Roseobacter lineage. Applied and Environmental Microbiology (2005) 71:5665.

Chet I, Mitchell R. Ecological aspects of microbial chemotactic behavior. Annual Reviews in Microbiology (1976) 30:221-239.

Cole JJ, Findlay S, Pace ML. Bacterial Production in Fresh and Saltwater Ecosystems - A Cross-System Overview. Mar. Ecol.-Prog. Ser. (1988) 43:1-10.

Croft MT, Lawrence AD, Raux-Deery E, Warren MJ, Smith AG. Algae acquire vitamin B 12 through a symbiotic relationship with bacteria. Nature (2005) 438:90-93.

Fuhrman JA, Azam F. Thymidine Incorporation as a Measure of Heterotrophic Bacterioplankton Production in Marine Surface Waters - Evaluation and Field Results. Mar. Biol. (1982) 66:109-120.

Goldman JC. Conceptual Role for Microaggregates in Pelagic Waters. Bull. Mar. Sci. (1984) 35:462-476.

Grossart HP, Riemann L, Azam F. Bacterial motility in the sea and its ecological implications. Aquat. Microb. Ecol. (2001) 25:247-258.

Guerrini F, Mazzotti A, Boni L, Pistocchi R. Bacterial-algal interactions in polysaccharide production. Aquat. Microb. Ecol. (1998) 15:247-253.

Guillard RR, Ryther JH. STUDIES OF MARINE PLANKTONIC DIATOMS .1. CYCLOTELLA NANA HUSTEDT, AND DETONULA CONFERVACEA (CLEVE) GRAN. Can. J. Microbiol. (1962) 8:229-&.

Jackson GA. Simulating Chemosensory Responses of Marine Microorganisms. Limnol. Oceanogr. (1987) 32:1253-1266.

Jackson GA. SIMULATION OF BACTERIAL ATTRACTION AND ADHESION TO FALLING PARTICLES IN AN AQUATIC ENVIRONMENT. Limnol. Oceanogr. (1989a) 34:514-530.

Jackson GA. Simulation of Bacterial Attraction and Adhesion to Falling Particles in Aquatic Environment. Limnol. Oceanogr. (1989b) 34:514-530.

Johansen JE, Pinhassi J, Blackburn N, Zweifel UL, Hagstrom A. Variability in motility characteristics among marine bacteria. Aquat. Microb. Ecol. (2002) 28:229-237.

Kiorboe T, Jackson GA. Marine snow, organic solute plumes, and optimal chemosensory behavior of bacteria. Limnol. Oceanogr. (2001) 46:1309-1318.

Koshland DE. Chemotaxis as a model for sensory systems. FEBS Letters (1974) 40:S3 - S9.

Krembs C, Juhl AR, Long RA, Azam F. Nanoscale Patchiness of Bacteria in Lake Water Studied with the Spatial Information Preservation Method. Limnol. Oceanogr. (1998) 43:307-314.

Larsen SH, Reader RW, Kort EN, Tso WW, Adler J. Change in Direction of Flagellar Rotation is Basis of Chemotactic Response in Escherichia-Coli. Nature (1974) 249:74-77.

Lehman JT, Scavia D. Microscale Patchiness of Nutrients in Plankton Communities. Science (1982) 216:729-730.

Locsei JT, Pedley TJ. Bacterial Tracking of Motile Algae Assisted by Algal Cell's Vorticity Field. Microb. Ecol. (2009) 58:63-74.

Luchsinger RH, Bergersen B, Mitchell JG. Bacterial swimming strategies and turbulence. Biophysical Journal (1999) 77:2377-2386.

Macnab RM, Koshland DE. Gradient-Sensing Mechanism in Bacterial Chemotaxis. Proceedings of the National Academy of Sciences of the United States of America (1972) 69:2509-&.

Mitchell JG. The influence of cell size on marine bacterial motility and energetics. Microb. Ecol. (1991) 22:227-238.

Mitchell JG, Okubo A, Fuhrman JA. Microzones Surrounding Phytoplankton form the Basis for a Stratified Marine Microbial Ecosystem. Nature (1985) 316:58-59.

MullerNiklas G, Agis M, Herndl GJ. Microscale distribution of bacterioplankton in relation to phytoplankton: Results from 100-nl samples. Limnol. Oceanogr. (1996) 41:1577-1582.

Parker MS, Armbrust EV. Synergistic Effects of Light, Temperature, and Nitrogen Source on Transcription of Genes for Carbon and Nitrogen Metabolism in the Centric Diatom Thalassiosira Pseudonana (Bacillariophyceae) 1. Journal of Phycology (2005) 41:1142-1153.

Polz MF, Hunt DE, Preheim SP, Weinreich DM. Patterns and mechanisms of genetic and phenotypic differentiation in marine microbes. Philosophical Transactions of the Royal Society B: Biological Sciences (2006) 361:2009.

Pomeroy LR, Williams PJI, Azam F, Hobbie JE. The Microbial Loop. Oceanography (2007) 20:28-33.

Purcell EM. Life at Low Reynolds-Number. Am. J. Phys. (1977) 45:3-11.

Rhee GY. Competition Between an Alga and an Aquatic Bacterium for Phosphate. Limnol. Oceanogr. (1972) 17:505-&.

Seymour JR, Ahmed T, Marcos RS. A microfluidic chemotaxis assay to study microbial behavior in diffusing nutrient patches. Limnol. Oceanogr. Methods (2008) 6:477-488.

Seymour JR, Stocker R. Resource patch formation and exploitation throughout the marine microbial food web. Am Nat (2009) 173:E15-E29

Seymour JR, Mitchell JG, Pearson L, Waters RL. Heterogeneity in bacterioplankton abundance from 4.5 millimetre resolution sampling. Aquat. Microb. Ecol. (2000) 22:143-153.

Seymour JR, Mitchell JG, Seuront L. Microscale heterogeneity in the activity of coastal bacterioplankton communities. Aquat. Microb. Ecol. (2004) 35:1-16.

Silverman M, Simon M. Flagellar rotation and the mechanism of bacterial motility. (1974).

Stocker R, Seymour JR, Samadani A, Hunt DE, Polz MF. Rapid chemotactic response enables marine bacteria to exploit ephemeral microscale nutrient patches. Proceedings of the National Academy of Sciences of the United States of America (2008) 105:4209-4214.

Tennekes H, Lumley JL. A first course in turbulence. (1972): The MIT press.

Tsang N, Macnab R, Koshland DE. Common Mechanism for Repellents and Attractants in Bacterial Chemotaxis. Science (1973) 181:60-63.